

1 DPHL v2: An updated and comprehensive DIA pan-human assay

2 library for quantifying more than 14,000 proteins

3
4 Zhangzhi Xue^{1,2,3}, Tiansheng Zhu^{1,2,3,15}, Fangfei Zhang^{1,2,3}, Cheng Zhang^{1,2,3}, Nan
5 Xiang⁴, Liuji Qian^{1,2,3}, Xiao Yi⁴, Yaoting Sun^{1,2,3}, Wei Liu⁴, Xue Cai^{1,2,3}, Linyan
6 Wang⁵, Xizhe Dai⁵, Liang Yue^{1,2,3}, Lu Li^{1,2,3}, Thang V. Pham⁶, Sander R.
7 Piersma⁶, Qi Xiao^{1,2,3}, Meng Luo⁷, Cong Lu⁸, Jiang Zhu⁸, Yongfu Zhao⁹,
8 Guangzhi Wang⁹, Junhong Xiao⁹, Tong Liu¹⁰, Zhiyu Liu¹¹, Yi He¹¹, Qijun Wu¹²,
9 Tingting Gong¹², Jianqin Zhu^{13,14}, Zhiguo Zheng^{13,14}, Juan Ye⁵, Yan Li⁷, Connie R.
10 Jimenez⁶*, Jun A^{1,2,3}*, Tiannan Guo^{1,2,3}*

11
12 ¹ iMarker lab, Westlake Laboratory of Life Sciences and Biomedicine, Key
13 Laboratory of Structural Biology of Zhejiang Province, School of Life Sciences,
14 Westlake University, Hangzhou, Zhejiang Province, China
15 ² Institute of Basic Medical Sciences, Westlake Institute for Advanced Study,
16 Hangzhou, Zhejiang Province, China
17 ³ Research Center for Industries of the Future, Westlake University, 600 Dunyu
18 Road, Hangzhou, Zhejiang, 310030, China
19 ⁴ Westlake Omics (Hangzhou) Biotechnology Co., Ltd., Hangzhou, China
20 ⁵ Department of Ophthalmology, The Second Affiliated Hospital, Zhejiang
21 University School of Medicine, Hangzhou, Zhejiang, China
22 ⁶ OncoProteomics Laboratory, Department of Medical Oncology, VU University
23 Medical Center, VU University, Amsterdam 1011, The Netherlands
24 ⁷ Songjiang research Institute and Songjiang Hospital, Department of Anatomy
25 and Physiology, College of Basic Medical Science,
26 Shanghai Jiao Tong University School of Medicine, Shanghai 201600, China
27 ⁸ Center for Stem Cell Research and Application, Union Hospital, Tongji Medical
28 College, Huazhong University of Science and Technology Wuhan, Hubei, P. R.
29 China
30 ⁹ Department of General Surgery, The Second Hospital of Dalian Medical
31 University, Dalian, China
32 ¹⁰ Harbin Medical University Cancer Hospital, Harbin 150081, Heilongjiang
33 Province, China

34 ¹¹ Department of Urology, The Second Hospital of Dalian Medical University,
35 No.467 Zhongshan Road, Dalian, Liaoning Province, China

36 ¹² Department of Clinical Epidemiology, Shengjing Hospital of China Medical
37 University, Shenyang 110000, Liaoning Province, China

38 ¹³ The Cancer Hospital of the University of Chinese Academy of Sciences
39 (Zhejiang Cancer Hospital), Hangzhou, Zhejiang, China

40 ¹⁴ Institute of Basic Medicine and Cancer (IBMC), Chinese Academy of Sciences,
41 Hangzhou, Zhejiang, China

42 ¹⁵ College of Mathematics and Computer Science, Zhejiang A & F University,
43 Hangzhou, China.

44
45 Correspondence: Connie Jimenez (c.jimenez@amsterdamumc.nl), Jun A
46 (ajun@westlake.edu.cn), Tiannan Guo (guotannan@westlake.edu.cn)

48 **Summary**

49 A comprehensive pan-human spectral library is critical for biomarker discovery
50 using mass spectrometry (MS)-based proteomics. DPHL v1, a previous pan-human
51 library built from 1096 data-dependent acquisition (DDA) MS data of 16 human
52 tissue types, allows quantifying 10,943 proteins. However, a major limitation of
53 DPHL v1 is the lack of semi-tryptic peptides and protein isoforms, which are
54 abundant in clinical specimens. Here, we generated DPHL v2 from 1608 DDA-MS
55 data acquired using Orbitrap mass spectrometers. The data included 586 DDA-MS
56 newly acquired from 17 tissue types, while 1022 files were derived from DPHL v1.
57 DPHL v2 thus comprises data from 24 sample types, including several cancer types
58 (lung, breast, kidney, and prostate cancer, among others). We generated four variants
59 of DPHL v2 to include semi-tryptic peptides and protein isoforms. DPHL v2 was then
60 applied to a publicly available colorectal cancer dataset with 286 DIA-MS files. The
61 numbers of identified and significantly dysregulated proteins increased by at least
62 21.7% and 14.2%, respectively, compared with DPHL v1. Our findings show that the
63 increased human proteome coverage of DPHL v2 provides larger pools of potential
64 protein biomarkers.

65

66 **Keywords**

67 Targeted proteomics; Spectral library; Data-independent acquisition; Mass
68 spectrometry; Cancer; Colorectal cancer

69

70 **Introduction**

71 Mass spectrometry (MS)-based quantitative proteomics is widely used for
72 protein biomarker discovery¹⁻³. The subsequent biomarker validation is often
73 performed with targeted proteomics methods, such as selected reaction monitoring
74 (SRM)⁴ and parallel reaction monitoring (PRM)⁵. Recently, biomarker discovery and
75 validation have been increasingly performed with targeted analysis of data-
76 independent acquisition (DIA) MS data⁶, an emerging strategy for high-throughput
77 proteomics analyses with a high level of reproducibility⁷. A spectral library containing
78 experimental peptide precursor information is crucial for SRM- and PRM-based
79 protein biomarker validation, as well as DIA-based biomarker discovery⁷. In recent
80 years, spectral libraries have been established for several organisms, such as human⁸,
81 mouse⁹, zebrafish¹⁰, *Arabidopsis thaliana*¹², and *Escherichia coli*¹³. To support the
82 identification of new protein biomarkers, the comprehensiveness of a spectral library
83 is crucial.

84 The Human Proteome Project (HPP)¹⁴ launched by Human Proteome
85 Organization (HUPO) has reported the community-based ten-year achievement of a
86 high-stringency proteome blueprint of 17,874 Protein Evidence 1 (PE1) proteins in
87 2020, covering 90.4% of the human proteome¹⁵. A pan-human spectral library (PHL),
88 containing 149,130 peptide precursors and 10,322 proteins, was developed to analyze
89 Sequential Window Acquisition of All Theoretical Mass Spectra (SWATH-MS) data
90 acquired on SCIEX TripleTOF Systems⁸. Another DIA pan-human library (DPHL v1)
91 for Orbitrap data comprises 289,237 peptide precursors and 10,943 proteins⁹.

92 However, the proteins in these two libraries are proteotypic; protein isoforms are not
93 included. The isoforms of each protein family may result from post-translational
94 modifications, splice variants, proteolytic products, genetic variations, or somatic
95 recombination occurring during protein evolution¹⁶, and participate in different
96 biological processes¹⁷. Therefore, a specific protein isoform could be a valuable
97 biomarker. A spectral library with significant coverage of the human proteome and its
98 protein isoforms is thus needed. Additionally, previous studies demonstrated that only
99 ~10-15% of all the tryptic peptides from a protein sample can be identified when
100 about 50% of the protein identifications are based on a single tryptic peptide due to
101 the intrinsic chemical properties of tryptic peptides¹⁸⁻²⁰. Therefore, identifying more
102 peptides (e.g., non-tryptic peptides), preferably at low computational costs, would
103 increase the confidence in the proteins identified via tryptic peptides and increase the
104 overall number of identifications.

105 Here, we present a large DIA spectral library (DPHL v2), generated from 24
106 different sample types and available in four variants. DPHL v2 includes more peptide
107 precursors, peptides, and proteins than DPHL v1. It also provides higher coverage
108 ratios, particularly for brain-, esophagus-, and ovary-specific or -enriched proteins, as
109 well as FDA-approved drug targets. Two variants of DPHL v2 generated better
110 identifications of the hallmark gene sets than DPHL v1. Finally, using a publicly
111 available colorectal cancer (CRC) cohort, DPHL v2 provided larger numbers of
112 protein and differentially expressed protein identifications than DPHL v1 and library-
113 free method.

114 **Results and Discussion**

115 **Data sources for generating DPHL v2**

116 A total of 1608 raw MS data files were collected to build our spectral library.

117 Among these, 586 files were newly generated from various samples, including tissue

118 biopsies of prostate cancer (PCa), hepatocellular carcinoma (HCC), triple-negative

119 breast cancer (TNBC), lung adenocarcinoma (LUAD), esophageal carcinoma, thyroid

120 diseases, eyelid tumors, glioblastoma multiforme (GBM), healthy brain tissues, oral

121 squamous cell carcinoma (OSCC), thymic diseases, ovarian cancer (OV), and cervix

122 cancer. Additionally, blood plasma samples from acute myelocytic leukemia (AML),

123 blood diseases, T-lineage acute lymphoblastic leukemia (T-ALL), and normal plasma

124 exosome were included. Human chronic myelogenous leukemia cell line K562 was

125 also included. Finally, the remaining 1022 files were derived from the DPHL v1 study

126 by Zhu *et al*⁹. The sample types and number of patients contributing to DPHL v2 are

127 summarized in Figure 1A and Table S1.

128 **Four variants of the pan-human spectral libraries**

129 All the 1608 raw files were centroided and converted into mzXML as previously

130 described⁹. These files were then combined to build our new spectral library. Two

131 different annotation files (i.e., reviewed and isoform-reviewed fasta files) were used

132 to search the mzXML spectra against two digestion modes (i.e., full-specific and

133 semi-specific) using MS-Fragger (version 3.0)²¹. The reviewed fasta file was obtained

134 from the UniProt database²² (accessed on 17 Jul. 2020); it included 20,361 reviewed

135 human proteins and was used as the reference. The isoform-reviewed annotation file

136 was also downloaded from UniProt (accessed on 5 Aug. 2020) and comprised 42,347
137 proteins, including 22,201 human isoforms. Philosopher²³ (version 3.2.9) was used for
138 library searching based on the spectra matches with a maximum of two missed
139 cleavages and a false discovery rate < 0.01 for spectra, peptides, and proteins. By
140 differently combining the two annotation files and the two digestion modes, we
141 generated four library variants: RF (reviewed fasta sequence & full-specific digestion
142 mode), RS (reviewed fasta sequence & semi-specific digestion mode), IF (isoform
143 fasta sequence & full-specific digestion mode), IS (isoform fasta sequence & semi-
144 specific digestion mode).

145 Next, in order to ensure the consistency of the results of different time gradients
146 of the mass spectrum, we used EasyPQP (version 0.1.9,
147 <https://github.com/grosenberger/easypqp>) to anchor the CiRT²¹ peptides for retention
148 time (RT) normalization. Quality controls (QC) were then performed using an R
149 script with the criteria next described to remove data of low quality. First, only
150 precursors with multiple fragments (≥ 2) and a normalized RT range from -60 to 200
151 were retained. Second, fragments with a library intensity < 10 or a precursor charge of
152 +1 were removed. Finally, peptides with only one precursor were retained. However,
153 when a peptide had two precursors, we kept the one with the highest intensity if the
154 absolute difference of the normalized RT between the two precursors was > 5;
155 otherwise, both precursors were kept. When a peptide has more than two precursors,
156 the averaged normalized RTs of all precursors and their differences with respect to
157 their mean RT were calculated. Next, peptides with an absolute difference > 5 were

158 excluded. When all the absolute values were > 5 , the median normalized RT of all the
159 precursors and their difference from the median RT were further calculated: only the
160 peptides with a difference < 5 were then selected. The normalized RT correlations
161 (+2/+3 states of each peptide) after these filtering steps are shown in Figure S1.

162 Default parameters were used for all software unless otherwise indicated. The
163 computational pipeline is schematized in Figure 1B.

164 **Characteristics of DPHL v2**

165 We next evaluated DPHL v2 using DIALib-QC²⁴ and found that all four variants
166 of our pan-human spectral library are of high quality (Figure S2-5). We also
167 characterized the four libraries in terms of peptide and protein identifications. As
168 shown in Figure 1C, the RF library includes 601,982 peptide precursors, 441,141
169 peptides, and 13,465 proteins; the IF library includes 604,748 peptide precursors,
170 443,150 peptides, and 14,375 proteins. IS, another isoform-based library, comprises
171 808,672 peptide precursors, 624,467 peptides, and 14,555 proteins. Finally, the RS
172 library contains 772,401 peptide precursors, 588,984 peptides, and 13,570 proteins.

173 We then evaluated the protein identifications of the four libraries for each of the 24
174 sample types. As shown in Figures S6-7, the brain had the highest number of total and
175 unique proteins among all sample types, possibly due to the larger number of brain
176 tissues included (n = 163).

177 Next, we compared our four libraries with the PHL and DPHL v1 and found that
178 our four libraries exhibited at least a 23.0% and 30.4% increase in protein coverage
179 compared to DPHL v1 and the PHL, respectively. Among our four libraries, the

180 isoform-based ones (IS and IF) comprise relatively high numbers of proteins (Figure
181 2A). Similarly, our four libraries exhibit considerably larger numbers of peptide
182 (Figure 2C) and precursor (Figure 2E) identifications when compared to DPHL v1
183 and the PHL. In particular, the semi-specific digestion libraries (IS and RS) have the
184 most significant numbers of peptide and precursor identifications. As shown in Figure
185 2B, 2D, and 2F, 7262 proteins, 89,328 peptides, and 103,704 precursors are shared
186 among these six libraries, while 1,144 proteins, 165,041 peptides, and 253,673
187 precursors are shared only by our four libraries. These findings indicate that DPHL v2
188 provides higher coverage among precursors, peptides, and proteins than DPHL v1 and
189 the PHL.

190 We next compared the numbers of shared proteins and peptides between our four
191 library variants (*i.e.*, between fasta files and digestion models) (Figure 3A, 3B). We
192 found that protein identifications were affected mainly by the fasta file, while peptide
193 identifications were affected by the digestion model. We also compared our four
194 libraries with DPHL v1 in terms of the enriched/specific proteins from three tissues
195 (brain, ovary, and esophagus; Figure 3C) obtained from the Human Protein Atlas
196 (<https://www.proteinatlas.org/>, data available from v21.0.proteinatlas.org). Our results
197 indicated that the coverages of our four libraries are superior to that of DPHL v1.
198 Similarly, our four libraries provided higher coverage of FDA-approved drug targets
199 than DPHL v1 (Figure 3C). In addition, the hallmark gene sets from the MSigDB v7.4
200 database (<http://www.broad.mit.edu/gsea/msigdb/>, accessed on 22 Nov. 2021)^{25, 26}
201 were analyzed using these five libraries. We found that RF and RS cover more than

202 44% of the genes with well-defined biological states or processes, and both provide
203 better coverages than DPHL v1 (Figure 3C). However, fewer coverages were found in
204 the isoform-based libraries. One possible reason is that most genes from the hallmark
205 gene sets are reviewed.

206 **Applicability of DPHL v2 for DIA targeted data analysis**

207 To assess the applicability of DPHL v2, we used our four libraries, DPHL v1, or
208 a library-free method to analyze a CRC cohort, including 201 CRC cases, 40 benign
209 samples, and 45 biological/technical replicates²⁷. The missing values generated by our
210 four libraries or DPHL v1 were comparable. On the other hand, the library-free
211 method generated fewer missing values (Figure 4A). As shown in Figure 4B, the
212 number of proteins identified with any variant of DPHL v2 was significantly higher
213 than with DPHL v1 or the library-free method. A total of 978 proteins were identified
214 by all six methods, while 166 were shared by our four libraries only (Figure 4C).

215 In order to demonstrate the applicability of the library, we performed differential
216 expression analyses of the CRC data generated using the six methods described
217 above. Differential expressions were considered significant if their adjusted p-values
218 were < 0.01 and their \log_2 (fold-change) absolute values were > 1 . We obtained 1997
219 (RF), 1984 (RS), 2024 (IF), 1992 (IS), 1783 (DPHL v1), and 1737 (library-free) up-
220 regulated (adjusted p-value < 0.01 & \log_2 (fold-change) > 1) proteins, and 330 (RF),
221 359 (RS), 346 (IF), 370 (IS), 255 (DPHL v1), and 230 (library-free) down-regulated
222 (adjust p-value < 0.01 & \log_2 (fold-change) < -1) proteins (Figure 4B). Compared
223 with the DPHL v1, the numbers of identified and significantly dysregulated proteins

224 increased by at least 21.7% (RF) and 14.2% (RF). Compared with the analysis using
225 only SwissProt reviewed proteins sequences, 463 and 472 differentially expressed
226 protein isoforms were identified using IF and IS, respectively. Similarly, 94 and 92
227 proteins were dysregulated in the CRC tissues compared with the benign samples by
228 semi-specific digestion modes. These findings show that DPHL v2 allows identifying
229 a larger number of differentially expressed proteins or protein isoforms between
230 tumors and benign samples, providing more options for subsequent investigations.

231 We next used our four libraries and DPHL v1 to analyze the CRC cohort using
232 the sub-library strategy²⁷, which refines a pan-human spectral library based on the
233 tissue specificity. Compared with the conventional library search method, the sub-
234 library strategy improved our results in all aspects (Figure S8A-C). First, the missing
235 values were reduced by about 1% on average. The protein identifications increased by
236 22 (RF), 344 (RS), 103 (IF), 405 (IS), or 193 (DPHL v1). In the subsequent
237 differential expression analysis, the total number of dysregulated proteins increased
238 by 70 (RF), 163 (RS), 42 (IF), 203 (IS), and 20 (DPHL v1).

239 Finally, we built a random forest model based on the overlap dysregulated
240 proteins generated by the four libraries to find new biomarkers. The 241 samples with
241 1426 proteins were randomly divided into the training set (N = 200) and the test set
242 (N = 41). After a 5-fold cross validation, we identified 14 features that provided the
243 highest accuracy for colorectal cancer, including S100A11, CEACAM6, GARS1,
244 CDYL2, POTEKP, SCGN, SNCG, S100B, SCG2, NCAM1, OGN, CD81, COL28A1,
245 CNRIP1 (Figure 5A). The area under the curve (AUC) of the training set and the test

246 set achieved 1, 0.903 (Figure 5B), and the accuracy (ACC) achieved 0.988, 0.927,
247 respectively (Figure 5C). Among these, S100A11^{28, 29}, CEACAM6^{30, 31}, CDYL2³²,
248 SCGN³³, SNCG^{34, 35}, S100B³⁶, SCG2^{37, 38}, NCAM1³⁹, OGN⁴⁰, CD81⁴¹, CNRIP1⁴²,
249 have been reported to be closely related to colorectal cancer. Three features (GARS1,
250 POTEKP, COL28A1) may be new biomarkers for colorectal cancer.

251 **Analysis of protein isoforms and semi-tryptic peptides**

252 We next checked whether this resource could be used to analyze specific protein
253 isoform. Among the dysregulated proteins from IF, we identified SPTBN1
254 (SPTBN1-long) and one of its isoforms (SPTBN1-short)⁴³. As reported in literature,
255 SPTBN1 is significantly dysregulated and plays an essential role in liver cancer⁴⁴,
256 colorectal cancer, and breast cancer, among others^{45, 46}. To assess the accuracy of the
257 identification, we showed the sequence of SPTBN1-long and SPTBN1-short
258 identified in the library, in addition to the common parts of the two sequences, our
259 library had also identified the peptide (TSSISGPLSPAYTGQVPYNYNQLEGR)
260 specific in SPTBN1-short (Figure 6A). The Skyline software (Skyline-daily version)
261 was used to show the peak spectrum of this peptide and a common peptide form these
262 two proteins within the DIA raw file (Figure 6B-C).

263 Regarding those were only characterized through semi-specific peptides in our
264 semi-specific libraries (IS and RS), including VWF, LMO7, ALDH2, NPEPL1,
265 NUAK1, and TPT1, many of them have important biologic implications. ADAM22 is
266 a new therapeutic option for treating metastatic brain disease and may be appropriate
267 for treatment of breast cancer^{47, 48}. By analyzing mRNA expression profiles, Xin et al.

268 found that *ASPM* is highly expressed in GBM, and patients with high *ASPM*
269 expression have poor prognoses⁴⁹. LRP6 inhibits cell proliferation and delays tumor
270 growth in vivo, especially in colon, liver, breast, and pancreatic cancers^{50, 51}. CHD9
271 was reported as a potential biomarker for clear cell renal cell carcinoma⁵². In addition,
272 FAIM2 promotes non-small cell lung cancer growth and bone metastasis formation by
273 regulating the epithelial-mesenchymal transformation process and the Wnt/β-catenin
274 signaling pathway⁵³. In our analysis, all these proteins showed significant differences
275 between tumor and non-tumor samples, indicating that DPHL v2 can assist with the
276 discovery of new potential protein biomarkers.

277 **Conclusion**

278 We present DPHL v2: four comprehensive spectral libraries (RF, RS, IF, and IS)
279 derived from 1608 DDA MS raw files, including 24 sample types. By identifying over
280 440,000 peptides and more than 14,000 proteins, DPHL v2 can confidently detect and
281 quantify more than 66.1% of the reviewed human proteins annotated by
282 UniProtKB/Swiss-Prot. Our results suggest that DPHL v2 could support protein
283 biomarker identification, especially for protein isoforms and semi-trypic peptides.
284 DPHL v2 outperforms previous DIA libraries in the following aspects. Firstly, five
285 additional tissue types (oral cavity, thymus, esophagus, eyelid, and ovary) and one
286 blood plasma sample from T-ALL were included. Secondly, protein isoforms and
287 semi-trypsin digestion were used for library searching. In addition, these libraries are
288 compatible with various commonly used DIA tools, with or without format
289 transformation, such as OpenSWATH⁵⁴, DIA-NN⁵⁵, Skyline⁵⁶, and Spectronaut⁵⁷.

290 **Materials and Methods**

291 All chemicals used in this study were purchased from Sigma. All MS-grade
292 reagents were acquired from Thermo Fisher Scientific (Waltham, MA).

293 **Clinical samples**

294 Formalin-fixed paraffin-embedded, fresh or fresh frozen tissue biopsies from
295 GBM, healthy human brain, eyelid tumor, thyroid disease, sarcoma, OSCC, thymus,
296 LUAD, TNBC, HCC, gastric cancer, diffuse large B-cell lymphoma, pancreatic ductal
297 adenocarcinoma, bladder cancer, PCa, and OV were collected in this study. Human
298 plasma samples, including acute lymphoblastic leukemia (ALL), AML, T-ALL,
299 normal plasma exosome, and blood disease, were also analyzed, as well as K562
300 cells. Six of these tissues were new additions compared to the DPHL v1. Eyelid
301 samples were obtained from the Second Affiliated Hospital of Zhejiang University
302 School of Medicine, China. The ovary cohort was obtained from The Cancer Hospital
303 of the University of Chinese Academy of Sciences. The OSCC, esophagus, T-ALL,
304 and thymus cancer samples were collected at Amsterdam UMC/VU Medical Center,
305 Amsterdam, and Erasmus University Medical Center. Sample details are provided in
306 Table S1.

307 To compare our libraries with the DPHL v1 and library-free method, we used the
308 DIA data of a CRC cohort generated by Ge et al.²⁷, which consists of 201 cancer
309 samples, 40 para-cancer tissues, and 45 biological and technical replicates from 40
310 CRC patients and four healthy controls. The detailed sample information is given in
311 Table S2.

312 **MS Data acquisition**

313 Among the newly added 586 DDA raw data files, 108 were derived from Dutch
314 cohorts generated at the Jimenez lab and 404 from Chinese cohorts generated at the
315 Guo lab. The pipeline for generating these DDA files coincided with that used for the
316 DPHL v1. The DDA raw files were centroided and converted into mzXML using
317 ProteoWizard⁵⁸ (version 3.0.11579). Carbamidomethylation was set as fixed
318 modification at cysteine residues; oxidation was set as variable modification at
319 methionine residues.

320 **DIA data analysis**

321 The DIA raw files were submitted to DIA-NN (1.7.15), a tool for DIA or
322 SWATH proteomics data analysis⁵⁵. Our four libraries were used as a reference, and
323 no other fasta sequences were added. The library inference was set to “off”. All other
324 parameters were kept to their default values. The tools we used for the DIA data
325 analysis, as described above, are publicly available⁵⁵.

326 **Machine learning**

327 The random forest analysis was performed with the R package “randomForest”
328 (version 4.6.14). 1426 proteins were firstly selected as input features to build 1000
329 trees with 5-fold cross validation and repeated 10 times to optimize the model. The
330 Mean Decrease Accuracy was set 4 to 6, with step size of 0.5. The final performance
331 was evaluated by mean accuracy (ACC) and mean area under curve (AUC) in a
332 receiver operating characteristic curve across 5-folds.

333 **Ethical statement**

334 Ethics approvals for this study were obtained from the Ethics Committee or
335 Institutional Review Board of each participating institution.

336 **Acknowledgments**

337 This work is supported by grants from National Key R&D Program of China
338 (2021YFA1301603; 2021YFA1301602; 2020YFE0202200).

339 **Author contributions**

340 T.G. conceived the project. Z.X. and T.Z. built all the libraries. Z.X. processed
341 and analyzed data. T.G., Z.X., T.Z., J.A., and F.Z. wrote the manuscript. Y.L.
342 collected the brain samples. J.Y. provided the eyelid tumor samples. T.L. offered the
343 lung cancer samples. J.Z. and C.L. collected the liver cancer samples. Y.H. offered
344 the prostate cancer samples. Q.W. provided the cervix cancer samples. J.Z. and Z.Z.
345 collected the ovarian cancer samples. Others prepared peptides for the study. T.G.
346 supervised the work. All authors reviewed and approved the manuscript.

347 **Competing interests**

348 T.G. is shareholder of Westlake Omics Inc. N.X., X.Y. and W.L. are employees
349 of Westlake Omics Inc. The other authors declare no competing interests in this
350 paper.

351 **Data Availability**

352 All newly added raw DDA MS data, spectral libraries, and protein results are
353 publicly available at iProX⁵⁹ (PXD015314) and ProteomeXchange (PXD015314). All
354 the R scripts were uploaded to GitHub (<https://github.com/zhtiansheng/DPHLv2>).

355 **References**

356 [1] Y. Zhu, R. Aebersold, M. Mann, T. Guo. (2021). SnapShot: Clinical proteomics,
357 Cell, 184, 4840-4840 e4841. <https://doi.org/10.1016/j.cell.2021.08.015>.

358 [2] Q. Xiao, F. Zhang, L. Xu, L. Yue, O.L. Kon, Y. Zhu, T. Guo. (2021). High-
359 throughput proteomics and AI for cancer biomarker discovery, Adv Drug Deliv Rev,
360 176, 113844. <https://doi.org/10.1016/j.addr.2021.113844>.

361 [3] R. Aebersold, M. Mann. (2016). Mass-spectrometric exploration of proteome
362 structure and function, Nature, 537, 347-355. <https://doi.org/10.1038/nature19949>.

363 [4] V. Lange, P. Picotti, B. Domon, R. Aebersold. (2008). Selected reaction monitoring
364 for quantitative proteomics: a tutorial, Mol Syst Biol, 4, 222.
365 <https://doi.org/10.1038/msb.2008.61>.

366 [5] A.C. Peterson, J.D. Russell, D.J. Bailey, M.S. Westphall, J.J. Coon. (2012). Parallel
367 reaction monitoring for high resolution and high mass accuracy quantitative, targeted
368 proteomics, Mol Cell Proteomics, 11, 1475-1488.
369 <https://doi.org/10.1074/mcp.O112.020131>.

370 [6] L.C. Gillet, P. Navarro, S. Tate, H. Rost, N. Selevsek, L. Reiter, R. Bonner, R.
371 Aebersold. (2012). Targeted data extraction of the MS/MS spectra generated by data-
372 independent acquisition: a new concept for consistent and accurate proteome analysis,
373 Mol Cell Proteomics, 11, O111.016717. <https://doi.org/10.1074/mcp.O111.016717>.

374 [7] F. Zhang, W. Ge, G. Ruan, X. Cai, T. Guo. (2020). Data-Independent Acquisition
375 Mass Spectrometry-Based Proteomics and Software Tools: A Glimpse in 2020,
376 Proteomics, 20, e1900276. <https://doi.org/10.1002/pmic.201900276>.

377 [8] G. Rosenberger, C.C. Koh, T. Guo, H.L. Rost, P. Kouvolanen, B.C. Collins, M. Heusel,
378 Y. Liu, E. Caron, A. Vichalkovski, M. Faini, O.T. Schubert, P. Faridi, H.A. Ebhardt, M.
379 Matondo, H. Lam, S.L. Bader, D.S. Campbell, E.W. Deutsch, R.L. Moritz, S. Tate, R.
380 Aebersold. (2014). A repository of assays to quantify 10,000 human proteins by
381 SWATH-MS, Sci Data, 1, 140031. <https://doi.org/10.1038/sdata.2014.31>.

382 [9] T. Zhu, Y. Zhu, Y. Xuan, H. Gao, X. Cai, S.R. Piersma, T.V. Pham, T. Schelfhorst,
383 R. Haas, I.V. Bijnsdorp, R. Sun, L. Yue, G. Ruan, Q. Zhang, M. Hu, Y. Zhou, W.J. Van
384 Houdt, T.Y.S. Le Large, J. Cloos, A. Wojtuszkiewicz, D. Koppers-Lalic, F. Bottger, C.
385 Scheepbouwer, R.H. Brakenhoff, G. van Leenders, J.N.M. Ijzermans, J.W.M. Martens,
386 R.D.M. Steenbergen, N.C. Grieken, S. Selvarajan, S. Mantoo, S.S. Lee, S.J.Y. Yeow,
387 S.M.F. Alkaff, N. Xiang, Y. Sun, X. Yi, S. Dai, W. Liu, T. Lu, Z. Wu, X. Liang, M. Wang,
388 Y. Shao, X. Zheng, K. Xu, Q. Yang, Y. Meng, C. Lu, J. Zhu, J. Zheng, B. Wang, S. Lou,
389 Y. Dai, C. Xu, C. Yu, H. Ying, T.K. Lim, J. Wu, X. Gao, Z. Luan, X. Teng, P. Wu, S.
390 Huang, Z. Tao, N.G. Iyer, S. Zhou, W. Shao, H. Lam, D. Ma, J. Ji, O.L. Kon, S. Zheng,
391 R. Aebersold, C.R. Jimenez, T. Guo. (2020). DPHL: A DIA Pan-human Protein Mass
392 Spectrometry Library for Robust Biomarker Discovery, Genomics Proteomics
393 Bioinformatics, 18, 104-119. <https://doi.org/10.1016/j.gpb.2019.11.008>.

394 [10] T. Lu, L. Qian, Y. Xie, Q. Zhang, W. Liu, W. Ge, Y. Zhu, L. Ma, C. Zhang, T. Guo.
395 (2022). Tissue-Characteristic Expression of Mouse Proteome, Mol Cell Proteomics, 21,
396 100408. <https://doi.org/10.1016/j.mcpro.2022.100408>.

397 [11] P. Blattmann, V. Stutz, G. Lizzo, J. Richard, P. Gut, R. Aebersold. (2019).

398 Generation of a zebrafish SWATH-MS spectral library to quantify 10,000 proteins, Sci
399 Data, 6, 190011. <https://doi.org/10.1038/sdata.2019.11>.

400 [12] H. Zhang, P. Liu, T. Guo, H. Zhao, D. Bensaddek, R. Aebersold, L. Xiong. (2019).
401 Arabidopsis proteome and the mass spectral assay library, Sci Data, 6, 278.
402 <https://doi.org/10.1038/s41597-019-0294-0>.

403 [13] M.K. Midha, U. Kusebauch, D. Shteynberg, C. Kapil, S.L. Bader, P.J. Reddy, D.S.
404 Campbell, N.S. Baliga, R.L. Moritz. (2020). A comprehensive spectral assay library to
405 quantify the Escherichia coli proteome by DIA/SWATH-MS, Sci Data, 7, 389.
406 <https://doi.org/10.1038/s41597-020-00724-7>.

407 [14] G.S. Omenn, L. Lane, C.M. Overall, C. Pineau, N.H. Packer, I.M. Cristea, C.
408 Lindskog, S.T. Weintraub, S. Orchard, M.H.A. Roehrl, E. Nice, S. Liu, N. Bandeira,
409 Y.J. Chen, T. Guo, R. Aebersold, R.L. Moritz, E.W. Deutsch. (2022). The 2022 Report
410 on the Human Proteome from the HUPO Human Proteome Project, J Proteome Res.
411 <https://doi.org/10.1021/acs.jproteome.2c00498>.

412 [15] S. Adhikari, E.C. Nice, E.W. Deutsch, L. Lane, G.S. Omenn, S.R. Pennington, Y.K.
413 Paik, C.M. Overall, F.J. Corrales, I.M. Cristea, J.E. Van Eyk, M. Uhlen, C. Lindskog,
414 D.W. Chan, A. Bairoch, J.C. Waddington, J.L. Justice, J. LaBaer, H. Rodriguez, F. He,
415 M. Kostrzewa, P. Ping, R.L. Gundry, P. Stewart, S. Srivastava, S. Srivastava, F.C.S.
416 Nogueira, G.B. Domont, Y. Vandenbrouck, M.P.Y. Lam, S. Wennersten, J.A. Vizcaino,
417 M. Wilkins, J.M. Schwenk, E. Lundberg, N. Bandeira, G. Marko-Varga, S.T. Weintraub,
418 C. Pineau, U. Kusebauch, R.L. Moritz, S.B. Ahn, M. Palmblad, M.P. Snyder, R.
419 Aebersold, M.S. Baker. (2020). A high-stringency blueprint of the human proteome,
420 Nat Commun, 11, 5301. <https://doi.org/10.1038/s41467-020-19045-9>.

421 [16] M. Uhlen, L. Fagerberg, B.M. Hallstrom, C. Lindskog, P. Oksvold, A. Mardinoglu,
422 A. Sivertsson, C. Kampf, E. Sjostedt, A. Asplund, I. Olsson, K. Edlund, E. Lundberg,
423 S. Navani, C.A. Szigyarto, J. Odeberg, D. Djureinovic, J.O. Takanen, S. Hober, T. Alm,
424 P.H. Edqvist, H. Berling, H. Tegel, J. Mulder, J. Rockberg, P. Nilsson, J.M. Schwenk,
425 M. Hamsten, K. von Feilitzen, M. Forsberg, L. Persson, F. Johansson, M. Zwahlen, G.
426 von Heijne, J. Nielsen, F. Ponten. (2015). Proteomics. Tissue-based map of the human
427 proteome, Science, 347, 1260419. <https://doi.org/10.1126/science.1260419>.

428 [17] M. Stastna, J.E. Van Eyk. (2012). Analysis of protein isoforms: can we do it better?,
429 Proteomics, 12, 2937-2948. <https://doi.org/10.1002/pmic.201200161>.

430 [18] P. Mallick, M. Schirle, S.S. Chen, M.R. Flory, H. Lee, D. Martin, J. Ranish, B.
431 Raught, R. Schmitt, T. Werner, B. Kuster, R. Aebersold. (2007). Computational
432 prediction of proteotypic peptides for quantitative proteomics, Nat Biotechnol, 25, 125-
433 131. <https://doi.org/10.1038/nbt1275>.

434 [19] H. Tang, R.J. Arnold, P. Alves, Z. Xun, D.E. Clemmer, M.V. Novotny, J.P. Reilly,
435 P. Radivojac. (2006). A computational approach toward label-free protein quantification
436 using predicted peptide detectability, Bioinformatics, 22, e481-488.
437 <https://doi.org/10.1093/bioinformatics/btl237>.

438 [20] D.J. States, G.S. Omenn, T.W. Blackwell, D. Fermin, J. Eng, D.W. Speicher, S.M.
439 Hanash. (2006). Challenges in deriving high-confidence protein identifications from
440 data gathered by a HUPO plasma proteome collaborative study, Nature Biotechnology,
441 24, 333-338. <https://doi.org/10.1038/nbt1183>.

442 [21] A.T. Kong, F.V. Leprevost, D.M. Avtonomov, D. Mellacheruvu, A.I. Nesvizhskii.
443 (2017). MSFragger: ultrafast and comprehensive peptide identification in mass
444 spectrometry-based proteomics, Nat Methods, 14, 513-520.
445 <https://doi.org/10.1038/nmeth.4256>.

446 [22] M. Magrane, C. UniProt. (2011). UniProt Knowledgebase: a hub of integrated
447 protein data, Database (Oxford), 2011, bar009. <https://doi.org/10.1093/database/bar009>.

448 [23] F. da Veiga Leprevost, S.E. Haynes, D.M. Avtonomov, H.Y. Chang, A.K.
449 Shanmugam, D. Mellacheruvu, A.T. Kong, A.I. Nesvizhskii. (2020). Philosopher: a
450 versatile toolkit for shotgun proteomics data analysis, Nat Methods, 17, 869-870.
451 <https://doi.org/10.1038/s41592-020-0912-y>.

452 [24] M.K. Midha, D.S. Campbell, C. Kapil, U. Kusebauch, M.R. Hoopmann, S.L.
453 Bader, R.L. Moritz. (2020). DIALib-QC an assessment tool for spectral libraries in
454 data-independent acquisition proteomics, Nat Commun, 11, 5251.
455 <https://doi.org/10.1038/s41467-020-18901-y>.

456 [25] T.P. Subramanian A, Mootha VK, Mukherjee S, Ebert BL, Gillette MA, Paulovich
457 A, Pomeroy SL, Golub TR, Lander ES, Mesirov JP. . Gene set enrichment analysis a
458 knowledge-based approach for interpreting genome-wide expression profiles, Proc Natl
459 Acad Sci U S A, 102. <https://doi.org/10.1073/pnas.0506580102>.

460 [26] A. Liberzon, C. Birger, H. Thorvaldsdottir, M. Ghandi, J.P. Mesirov, P. Tamayo.
461 (2015). The Molecular Signatures Database (MSigDB) hallmark gene set collection,
462 Cell Syst, 1, 417-425. <https://doi.org/10.1016/j.cels.2015.12.004>.

463 [27] W. Ge, X. Liang, F. Zhang, Y. Hu, L. Xu, N. Xiang, R. Sun, W. Liu, Z. Xue, X. Yi,
464 Y. Sun, B. Wang, J. Zhu, C. Lu, X. Zhan, L. Chen, Y. Wu, Z. Zheng, W. Gong, Q. Wu,
465 J. Yu, Z. Ye, X. Teng, S. Huang, S. Zheng, T. Liu, C. Yuan, T. Guo. (2021).
466 Computational Optimization of Spectral Library Size Improves DIA-MS Proteome
467 Coverage and Applications to 15 Tumors, J Proteome Res, 20, 5392-5401.
468 <https://doi.org/10.1021/acs.jproteome.1c00640>.

469 [28] A.J. Guo, F.J. Wang, Q. Ji, H.W. Geng, X. Yan, L.Q. Wang, W.W. Tie, X.Y. Liu,
470 R.F. Thorne, G. Liu, A.M. Xu. (2021). Proteome Analyses Reveal S100A11, S100P,
471 and RBM25 Are Tumor Biomarkers in Colorectal Cancer, Proteomics Clin Appl, 15,
472 e2000056. <https://doi.org/10.1002/prca.202000056>.

473 [29] Y. Niu, Z. Shao, H. Wang, J. Yang, F. Zhang, Y. Luo, L. Xu, Y. Ding, L. Zhao.
474 (2016). LASP1-S100A11 axis promotes colorectal cancer aggressiveness by
475 modulating TGFbeta/Smad signaling, Sci Rep, 6, 26112.
476 <https://doi.org/10.1038/srep26112>.

477 [30] E. Ferlizza, R. Solmi, R. Miglio, E. Nardi, G. Mattei, M. Sgarzi, M. Lauriola.
478 (2020). Colorectal cancer screening: Assessment of CEACAM6, LGALS4, TSPAN8
479 and COL1A2 as blood markers in faecal immunochemical test negative subjects, J Adv
480 Res, 24, 99-107. <https://doi.org/10.1016/j.jare.2020.03.001>.

481 [31] M.T. Rodia, R. Solmi, F. Pasini, E. Nardi, G. Mattei, G. Ugolini, L. Ricciardiello,
482 P. Strippoli, R. Miglio, M. Lauriola. (2018). LGALS4, CEACAM6, TSPAN8, and
483 COL1A2: Blood Markers for Colorectal Cancer-Validation in a Cohort of Subjects With
484 Positive Fecal Immunochemical Test Result, Clin Colorectal Cancer, 17, e217-e228.
485 <https://doi.org/10.1016/j.clcc.2017.12.002>.

486 [32] S.I. Kim ST, DO IG, Jang J, Kim SH, Jung IH, Park JO, Park YS, Talasaz A, Lee
487 J, Kim HC. . (2014). Transcriptome analysis of CD133-positive stem cells and
488 prognostic value of survivin in colorectal cancer, *Cancer Genomics Proteomics*, 11,
489 259-266.

490 [33] X.Y. Yang, Q.R. Liu, L.M. Wu, X.L. Zheng, C. Ma, R.S. Na. (2018).
491 Overexpression of secretagogin promotes cell apoptosis and inhibits migration and
492 invasion of human SW480 human colorectal cancer cells, *Biomed Pharmacother*, 101,
493 342-347. <https://doi.org/10.1016/j.biopha.2018.01.147>.

494 [34] H. Hu, L. Sun, C. Guo, Q. Liu, Z. Zhou, L. Peng, J. Pan, L. Yu, J. Lou, Z. Yang, P.
495 Zhao, Y. Ran. (2009). Tumor cell-microenvironment interaction models coupled with
496 clinical validation reveal CCL2 and SNCG as two predictors of colorectal cancer
497 hepatic metastasis, *Clin Cancer Res*, 15, 5485-5493. <https://doi.org/10.1158/1078-0432.CCR-08-2491>.

499 [35] D.B. Liu C, Lu A, Qu L, Xing X, Meng L, Wu J, Eric Shi Y, Shou C. . (2010).
500 Synuclein gamma predicts poor clinical outcome in colon cancer with normal levels of
501 carcinoembryonic antigen, *BMC Cancer*, 359, 1471-2407.

502 [36] M.Y. Huang, H.M. Wang, T.S. Tok, H.J. Chang, M.S. Chang, T.L. Cheng, J.Y.
503 Wang, S.R. Lin. (2012). EVI2B, ATP2A2, S100B, TM4SF3, and OLFM4 as potential
504 prognostic markers for postoperative Taiwanese colorectal cancer patients, *DNA Cell
505 Biol*, 31, 625-635. <https://doi.org/10.1089/dna.2011.1365>.

506 [37] H. Wang, J. Yin, Y. Hong, A. Ren, H. Wang, M. Li, Q. Zhao, C. Jiang, L. Liu.
507 (2021). SCG2 is a Prognostic Biomarker Associated With Immune Infiltration and
508 Macrophage Polarization in Colorectal Cancer, *Front Cell Dev Biol*, 9, 795133.
509 <https://doi.org/10.3389/fcell.2021.795133>.

510 [38] S. Weng, Z. Liu, X. Ren, H. Xu, X. Ge, Y. Ren, Y. Zhang, Q. Dang, L. Liu, C. Guo,
511 R. Beatson, J. Deng, X. Han. (2022). SCG2: A Prognostic Marker That Pinpoints
512 Chemotherapy and Immunotherapy in Colorectal Cancer, *Front Immunol*, 13, 873871.
513 <https://doi.org/10.3389/fimmu.2022.873871>.

514 [39] T. Kok-Sin, N.M. Mokhtar, N.Z. Ali Hassan, I. Sagap, I. Mohamed Rose, R. Harun,
515 R. Jamal. (2015). Identification of diagnostic markers in colorectal cancer via
516 integrative epigenomics and genomics data, *Oncol Rep*, 34, 22-32.
517 <https://doi.org/10.3892/or.2015.3993>.

518 [40] X. Hu, Y.Q. Li, Q.G. Li, Y.L. Ma, J.J. Peng, S.J. Cai. (2018). Osteoglycin (OGN)
519 reverses epithelial to mesenchymal transition and invasiveness in colorectal cancer via
520 EGFR/Akt pathway, *J Exp Clin Cancer Res*, 37, 41. <https://doi.org/10.1186/s13046-018-0718-2>.

522 [41] H. Yuan, J. Zhao, Y. Yang, R. Wei, L. Zhu, J. Wang, M. Ding, M. Wang, Y. Gu.
523 (2020). SHP-2 Interacts with CD81 and Regulates the Malignant Evolution of
524 Colorectal Cancer by Inhibiting Epithelial-Mesenchymal Transition, *Cancer Manag
525 Res*, 12, 13273-13284. <https://doi.org/10.2147/CMAR.S270813>.

526 [42] T. Zhang, G. Cui, Y.L. Yao, Q.C. Wang, H.G. Gu, X.N. Li, H. Zhang, W.M. Feng,
527 Q.L. Shi, W. Cui. (2017). Value of CNRIP1 promoter methylation in colorectal cancer
528 screening and prognosis assessment and its influence on the activity of cancer cells,
529 *Arch Med Sci*, 13, 1281-1294. <https://doi.org/10.5114/aoms.2017.65829>.

530 [43] N.V. L., Hayes, Catherine Scott, Egidius Heerkens, Vasken Ohanian, Alison M.
531 Maggs, J. C., Pinder, Ekaterini Kordeli, A.J. Baines. (2000). Identification of a novel
532 C-terminal variant of β II spectrin two isoforms of β II spectrin have distinct intracellular
533 locations and activities, *Journal of Cell Science*, 113, 2023-2034.

534 [44] Shuyun Rao, Xiaochun Yang, Kazufumi Ohshiro, Sobia Zaidi, Zhanhuai Wang,
535 Kirti Shetty, Xiyang Xiang, Md. Imtaiyaz Hassan, Taj Mohammad, Patricia S. Latham,
536 Bao-Ngoc Nguyen, Linda Wong, Herbert Yu, Yousef Al-Abed, Bibhuti Mishra, Michele
537 Vacca, Gareth Guenigault, Michael E. D. Allison, Antonio Vidal-Puig, Jihane N.
538 Benhammou, Marcus Alvarez, Päivi Pajukanta, Joseph R. Pisegna, L. Mishra. (2021).
539 β 2-spectrin (SPTBN1) as a therapeutic target for diet-induced liver disease and
540 preventing cancer development, *SCIENCE TRANSLATIONAL MEDICINE*, 13.

541 [45] P. Yang, Y. Yang, P. Sun, Y. Tian, F. Gao, C. Wang, T. Zong, M. Li, Y. Zhang, T.
542 Yu, Z. Jiang. (2021). β II spectrin (SPTBN1): biological function and clinical
543 potential in cancer and other diseases, *Int J Biol Sci*, 17, 32-49.
544 <https://doi.org/10.7150/ijbs.52375>.

545 [46] Z.X. Yao, W. Jogunoori, S. Choufani, A. Rashid, T. Blake, W. Yao, P. Kreishman,
546 R. Amin, A.A. Sidawy, S.R. Evans, M. Finegold, E.P. Reddy, B. Mishra, R. Weksberg,
547 R. Kumar, L. Mishra. (2010). Epigenetic silencing of beta-spectrin, a TGF-beta
548 signaling/scaffolding protein in a human cancer stem cell disorder: Beckwith-
549 Wiedemann syndrome, *J Biol Chem*, 285, 36112-36120.
550 <https://doi.org/10.1074/jbc.M110.162347>.

551 [47] S. Charmsaz, B. Doherty, S. Cocchiglia, D. Vareslija, A. Marino, N. Cosgrove, R.
552 Marques, N. Priedigkeit, S. Purcell, F. Bane, J. Bolger, C. Byrne, P.J. O'Halloran, F.
553 Brett, K. Sheehan, K. Brennan, A.M. Hopkins, S. Keelan, P. Jagust, S. Madden, C.
554 Martinelli, M. Battaglini, S. Oesterreich, A.V. Lee, G. Ciofani, A.D.K. Hill, L.S. Young.
555 (2020). ADAM22/LGI1 complex as a new actionable target for breast cancer brain
556 metastasis, *BMC Med*, 18, 349. <https://doi.org/10.1186/s12916-020-01806-4>.

557 [48] J. Li, M. Lu, J. Jin, X. Lu, T. Xu, S. Jin. (2018). miR-449a Suppresses Tamoxifen
558 Resistance in Human Breast Cancer Cells by Targeting ADAM22, *Cell Physiol
559 Biochem*, 50, 136-149. <https://doi.org/10.1159/000493964>.

560 [49] Xin Chen, Lijie Huang, Yang Yang, Suhua Chen, Jianjun Sun, Changcheng Ma,
561 Jingcheng Xie, Yongmei Song, J. Yang. ASPM promotes glioblastoma growth by
562 regulating G1 restriction point progression and Wnt- β -catenin signaling, 224-241.

563 [50] J. Raisch, A. Cote-Biron, N. Rivard. (2019). A Role for the WNT Co-Receptor
564 LRP6 in Pathogenesis and Therapy of Epithelial Cancers, *Cancers (Basel)*, 11.
565 <https://doi.org/10.3390/cancers11081162>.

566 [51] J. Zhang, J. Chen, D. Wo, H. Yan, P. Liu, E. Ma, L. Li, L. Zheng, D. Chen, Z. Yu,
567 C. Liang, J. Peng, D.N. Ren, W. Zhu. (2019). LRP6 Ectodomain Prevents SDF-
568 1/CXCR4-Induced Breast Cancer Metastasis to Lung, *Clin Cancer Res*, 25, 4832-4845.
569 <https://doi.org/10.1158/1078-0432.CCR-18-3557>.

570 [52] Bo Guan, Xian-Gui Ran, Yong-Qiang Du, Feng Ren4, Ye Tian, Ying Wang, M.-M.
571 Chen. (2018). High CHD9 expression is associated with poor prognosis in clear cell
572 renal cell carcinoma, *Int J Clin Exp Pathol*, 11, 3697-3702.

573 [53] K. She, W. Yang, M. Li, W. Xiong, M. Zhou. (2021). FAIM2 Promotes Non-Small

574 Cell Lung Cancer Cell Growth and Bone Metastasis by Activating the Wnt/beta-
575 Catenin Pathway, *Front Oncol*, 11, 690142. <https://doi.org/10.3389/fonc.2021.690142>.

576 [54] H.L. Rost, G. Rosenberger, P. Navarro, L. Gillet, S.M. Miladinovic, O.T. Schubert,
577 W. Wolski, B.C. Collins, J. Malmstrom, L. Malmstrom, R. Aebersold. (2014).
578 OpenSWATH enables automated, targeted analysis of data-independent acquisition MS
579 data, *Nat Biotechnol*, 32, 219-223. <https://doi.org/10.1038/nbt.2841>.

580 [55] V. Demichev, C.B. Messner, S.I. Vernardis, K.S. Lilley, M. Ralser. (2020). DIA-
581 NN: neural networks and interference correction enable deep proteome coverage in
582 high throughput, *Nat Methods*, 17, 41-44. <https://doi.org/10.1038/s41592-019-0638-x>.

583 [56] B. MacLean, D.M. Tomazela, N. Shulman, M. Chambers, G.L. Finney, B. Frewen,
584 R. Kern, D.L. Tabb, D.C. Liebler, M.J. MacCoss. (2010). Skyline: an open source
585 document editor for creating and analyzing targeted proteomics experiments,
586 *Bioinformatics*, 26, 966-968. <https://doi.org/10.1093/bioinformatics/btq054>.

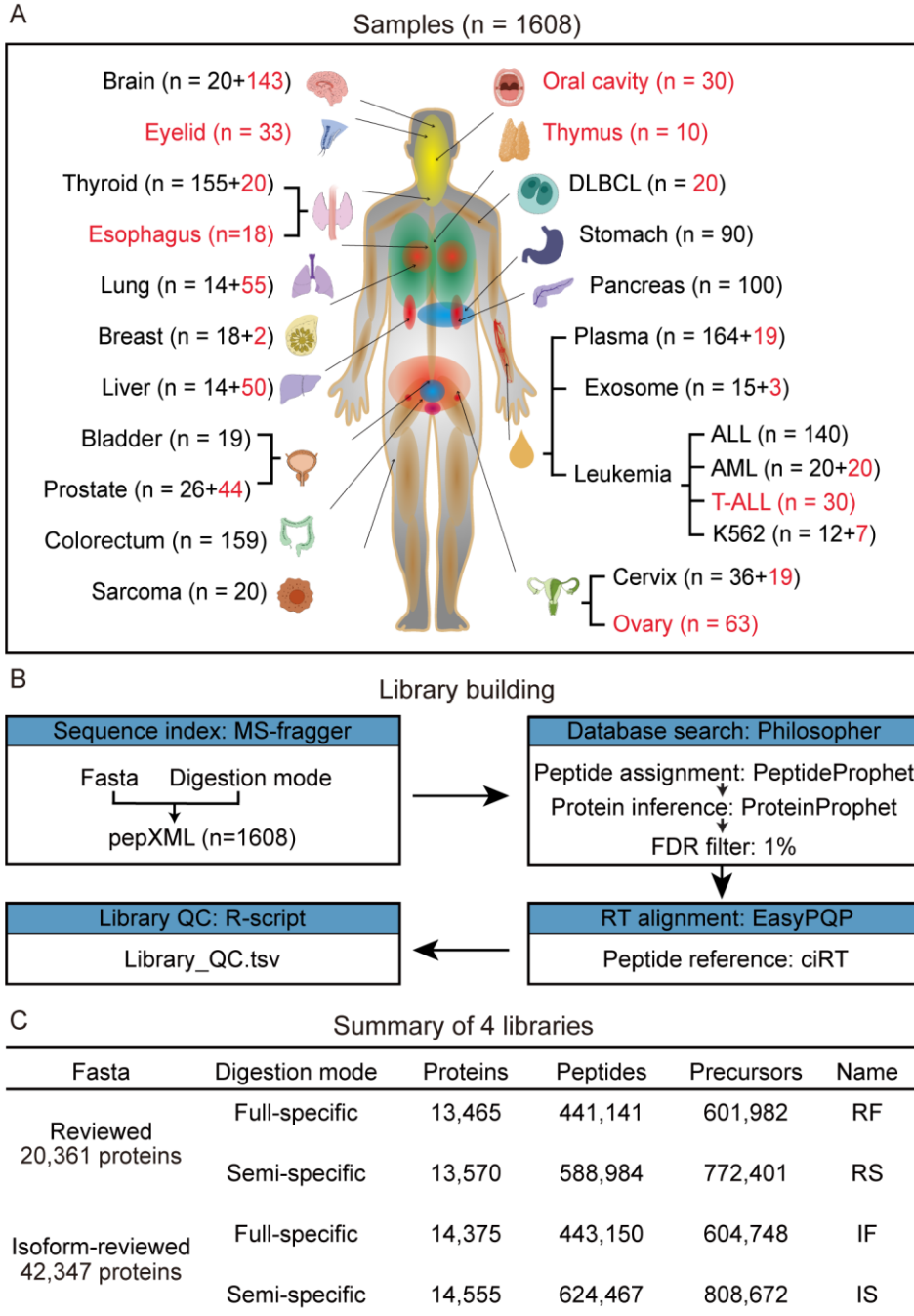
587 [57] Ana Martinez-Val, Dorte Breinholdt Bekker-Jensen, Alexander Hogrebe, J.V.
588 Olsen. (2021). Data Processing and Analysis for DIA-Based Phosphoproteomics Using
589 Spectronaut, *Proteomics Data Analysis, Methods in Molecular Biology*, 2361, 95-107.
590 https://doi.org/https://doi.org/10.1007/978-1-0716-1641-3_6.

591 [58] M.C. Chambers, B. Maclean, R. Burke, D. Amodei, D.L. Ruderman, S. Neumann,
592 L. Gatto, B. Fischer, B. Pratt, J. Egertson, K. Hoff, D. Kessner, N. Tasman, N. Shulman,
593 B. Frewen, T.A. Baker, M.Y. Brusniak, C. Paulse, D. Creasy, L. Flashner, K. Kani, C.
594 Moulding, S.L. Seymour, L.M. Nuwaysir, B. Lefebvre, F. Kuhlmann, J. Roark, P.
595 Rainer, S. Detlev, T. Hemenway, A. Huhmer, J. Langridge, B. Connolly, T. Chadick, K.
596 Holly, J. Eckels, E.W. Deutsch, R.L. Moritz, J.E. Katz, D.B. Agus, M. MacCoss, D.L.
597 Tabb, P. Mallick. (2012). A cross-platform toolkit for mass spectrometry and
598 proteomics, *Nat Biotechnol*, 30, 918-920. <https://doi.org/10.1038/nbt.2377>.

599 [59] J. Ma, T. Chen, S. Wu, C. Yang, M. Bai, K. Shu, K. Li, G. Zhang, Z. Jin, F. He, H.
600 Hermjakob, Y. Zhu. (2019). iProX: an integrated proteome resource, *Nucleic Acids Res*,
601 47, D1211-D1217. <https://doi.org/10.1093/nar/gky869>.

602
603
604
605
606
607
608
609
610
611
612
613
614
615
616
617

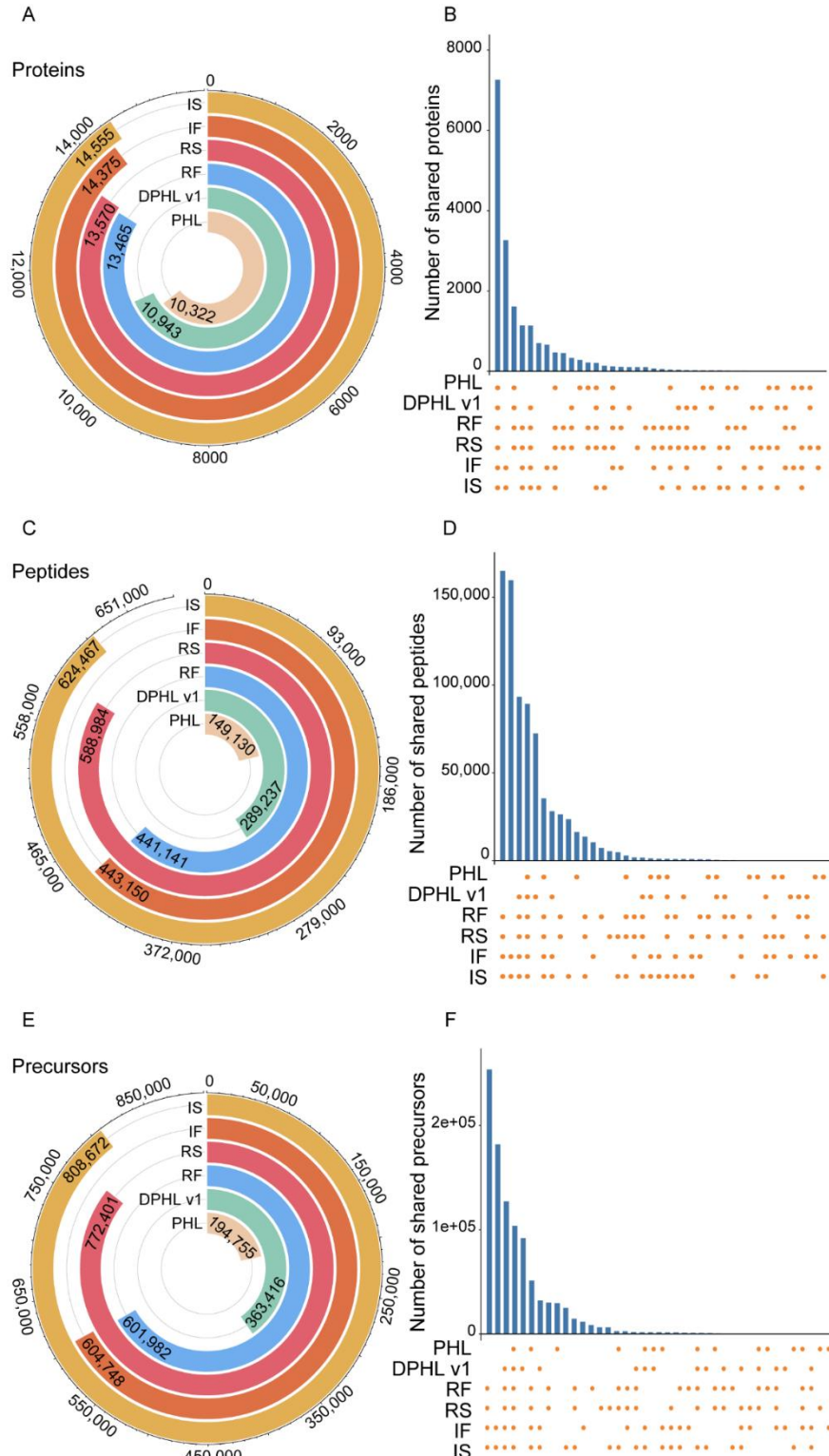
618 **Figure 1.**



619

620 **Figure 1. Sample types and workflow for building DPHL v2. (A)** Number and type
 621 of samples included in this study. The ones that were missing from DPHL v1 are
 622 highlighted in red. **(B)** Computational pipeline for building DPHL v2. **(C)** Overview
 623 of the number of identified proteins, peptides, and precursors using our four library
 624 variants.

625 **Figure 2.**



626

627 **Figure 2. Comparison of the four variants of DPHL v2 (i.e., RF, RS, IF, and IS)**

628 **with DPHL v1 and PHL.** The circular bars show the protein (A), peptide (C), and

629 precursor identifications (E) of the six libraries. The UpSet plots show the shared and

630 unique protein (B), peptide (D), and precursor identifications (F) of the six libraries.

631 PHL, pan-human spectral library; DPHL v1, DIA pan-human library generated by

632 Zhu *et al*; RF, reviewed fasta sequence & full-specific digestion mode; RS, reviewed

633 fasta sequence & semi-specific digestion mode; IF, isoform fasta sequence & full-

634 specific digestion mode; IS, isoform fasta sequence & semi-specific digestion mode.

635

636

637

638

639

640

641

642

643

644

645

646

647

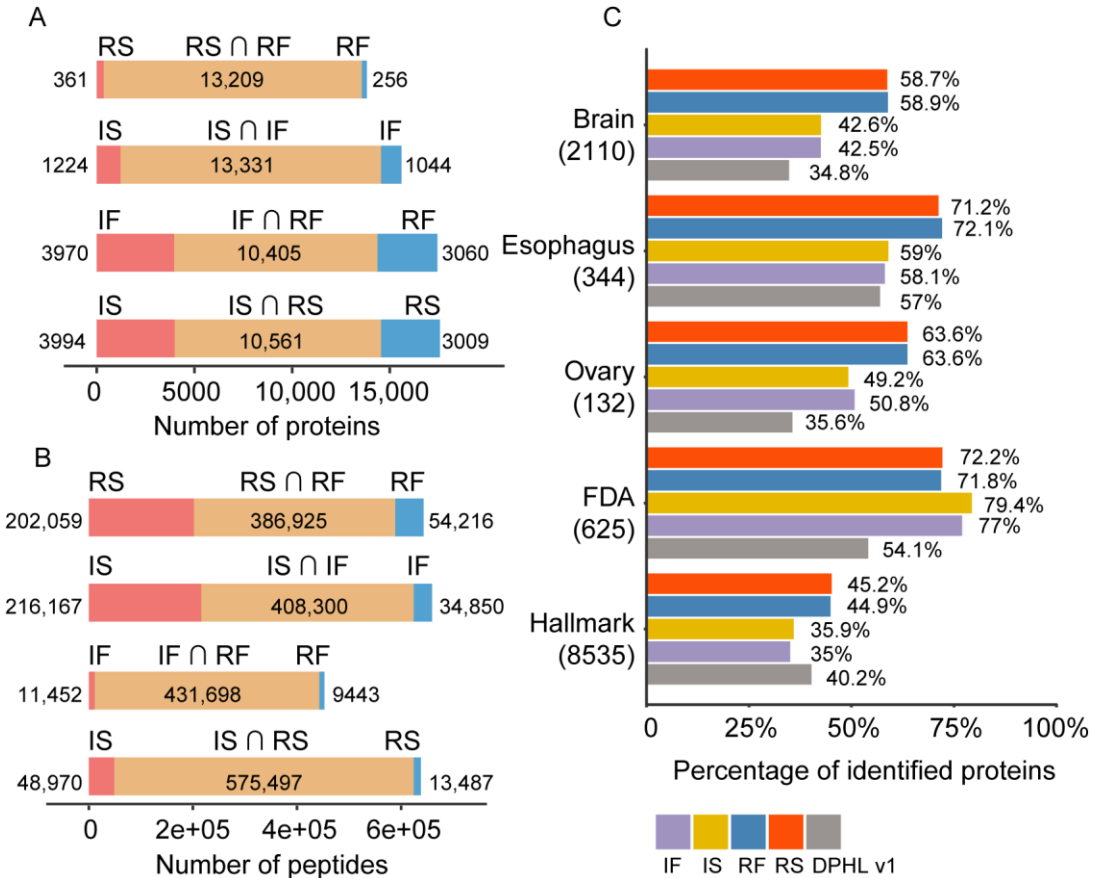
648

649

650

651

652 **Figure 3.**



653

654 **Figure 3.** Comparison of the number of proteins (A) and peptides (B) identified with
655 the same fasta sequence and the same digestion mode. (C) Percentage of proteins
656 identified among DPHL v1 and our four libraries using hallmark gene sets, FDA-
657 approved drug targets, and tissue-specific or tissue-enriched/enhanced proteins from
658 brain, esophagus, and ovary samples.

659

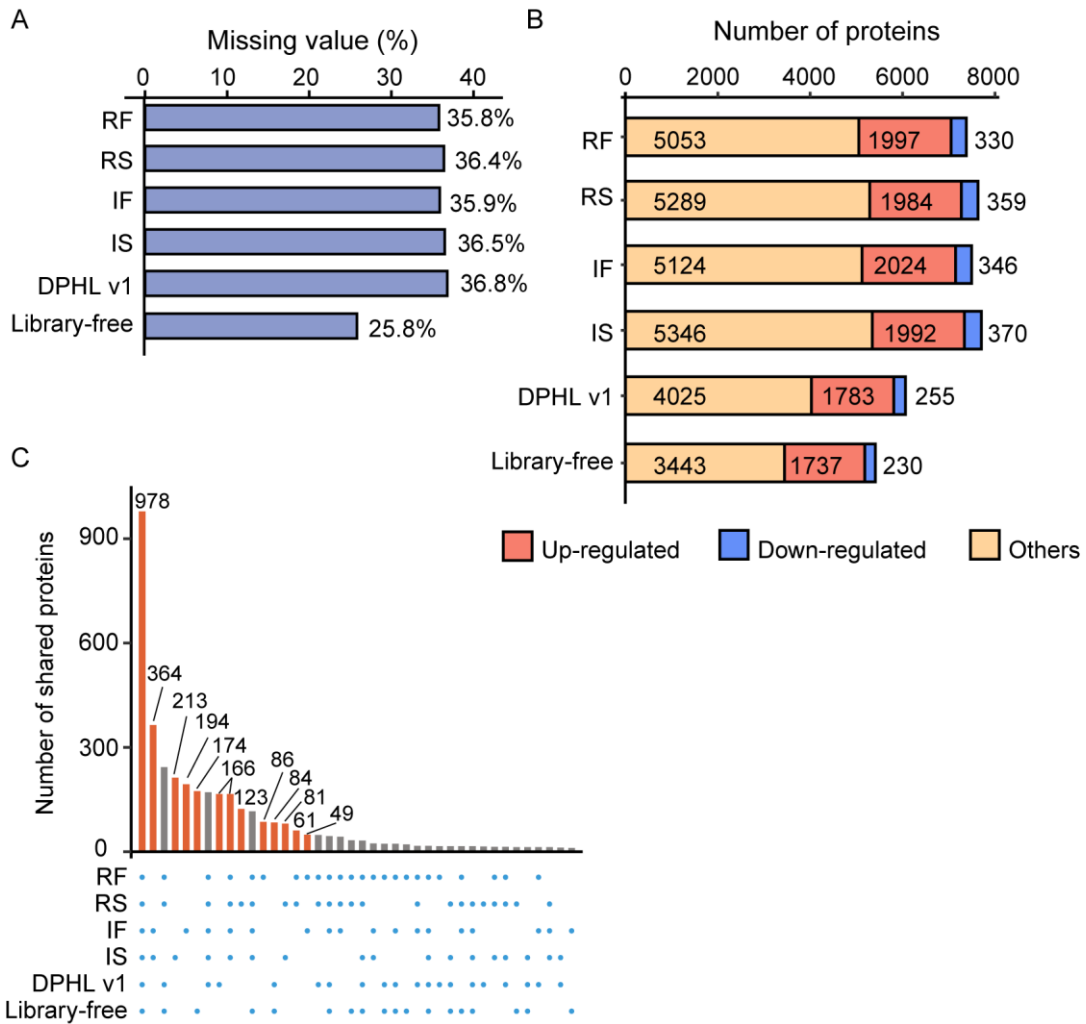
660

661

662

663

664 **Figure 4.**



665

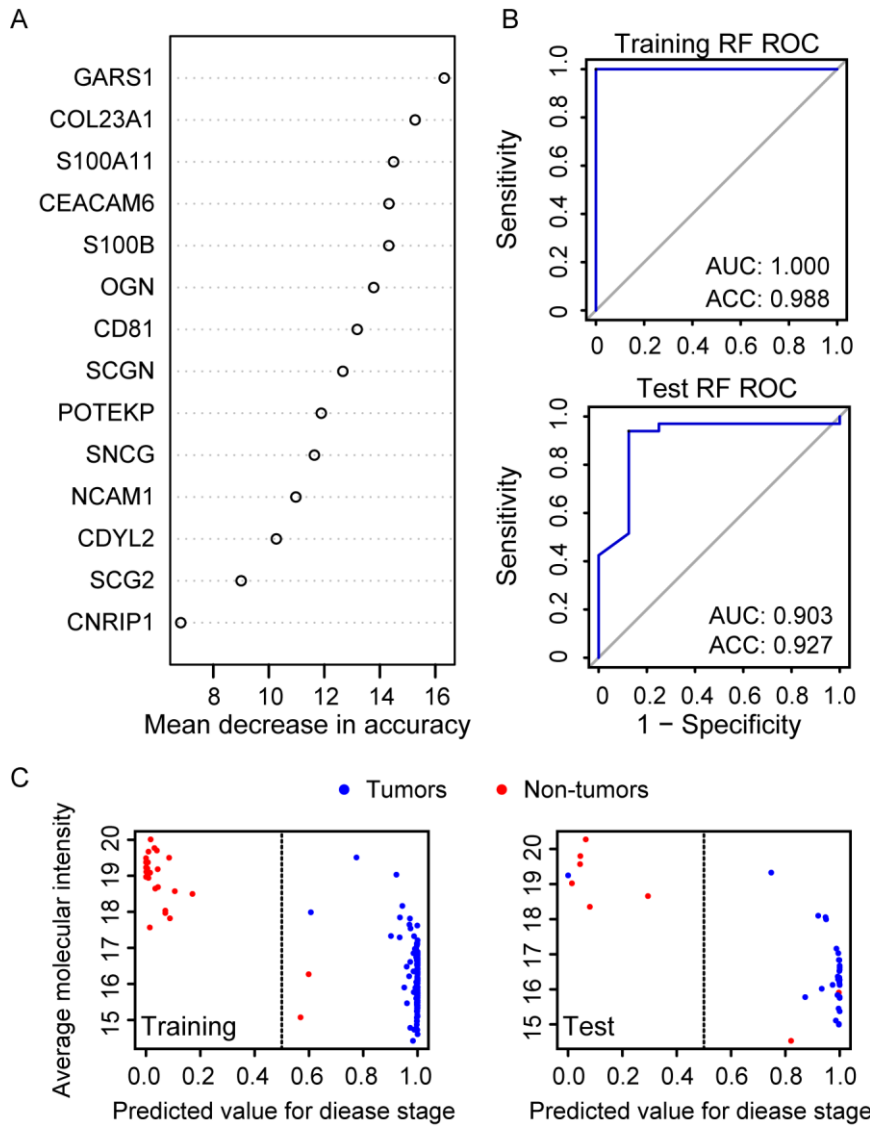
666 **Figure 4. DIA analysis of CRC and benign samples.** (A) Number of missing values
667 obtained using the five libraries and library-free method. (B) Number of differentially
668 expressed proteins between CRC and benign samples obtained using the five libraries
669 and library-free method. Proteins with adjusted p-value < 0.01 and $|FC| > 4$ were
670 selected as significantly differentially expressed. FC, fold change. (C) Protein
671 identification overlaps across the six libraries.

672

673

674

675 **Figure 5.**



676

677 **Figure 5. Machine learning to identify potential CRC biomarkers. (A)**

678 Prioritization of 14 important variables. (B) ROC plots for the training set (up) and

679 the test set (down). (C) Performance of the model in the training set and test set.

680

681

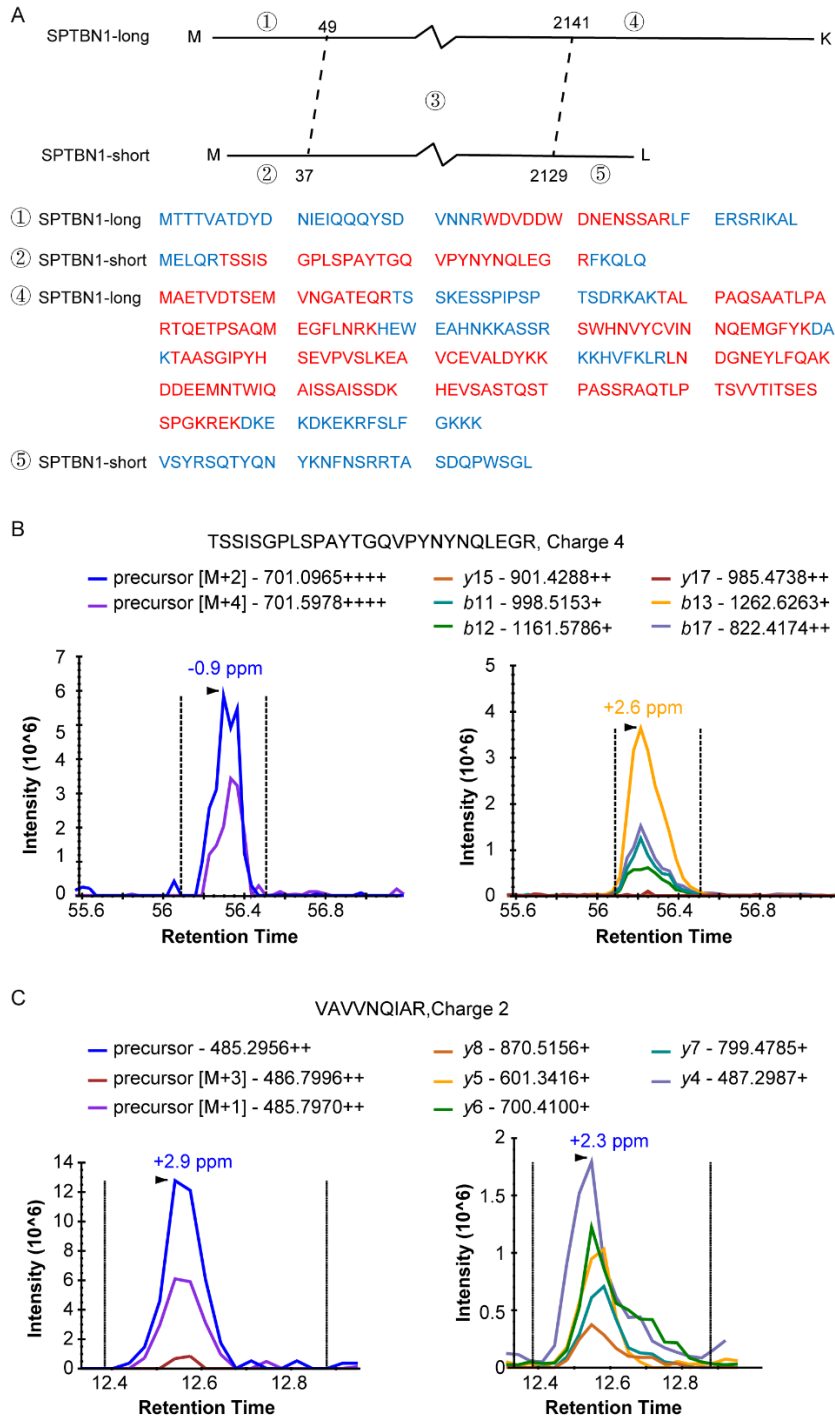
682

683

684

685

Figure 6.



686

687 **Figure 6. SPTBN1 protein identification in our DIA search results. (A) Sequences**
 688 of SPTBN1 and its isoform. Blue: sequences that were not identified; red: identified
 689 sequences. (B) The peak spectrum of peptide SSISGPLSPAYTGQVPYNNYNQLEGR
 690 in our DIA raw file (obtained using Skyline).